UNIVERSIDAD CARLOS III DE MADRID working papers

Working Paper 08 - 74
Statistics and Econometrics Series 27
December 2008

Departamento de Estadística
Universidad Carlos III de Madrid
Calle Madrid, 126
28903 Getafe (Spain)
Fax (34) 91 624-98-49

A FUNCTIONAL DATA BASED METHOD FOR TIME SERIES CLASSIFICATION

Andrés M. Alonso[1], David Casado[2], Sara López-Pintado[3] and Juan Romo[4]

Abstract

We propose using the integrated periodogram to classify time series. The method assigns a new element to the group minimizing the distance from the integrated periodogram of the element to the group mean of integrated periodograms. Local computation of these periodograms allows the application of the approach to non--stationary time series. Since the integrated periodograms are functional data, we apply depth-based techniques to make the classification robust. The method provides small error rates with both simulated and real data, and shows good computational behaviour.

Keywords: time series, classification, integrated periodogram, data depth

JEL Classification: C14 and C22

[1] Departamento de Estadística. Universidad Carlos III de Madrid, C/ Madrid 126, 28903 Getafe (Madrid), e-mail: andres.alonso@uc3m.es
[2] Departamento de Estadística. Universidad Carlos III de Madrid, C/ Madrid 126, 28903 Getafe (Madrid), e-mail: david.casado@uc3m.es
[3] Departamento de Economía, Métodos Cuantitativos e Historia Económica. Universidad Pablo de Olavide, Ctra. de Utrera, Km.1 - 41013 Sevilla, email: sloppin@upo.es
[4] Departamento de Estadística. Universidad Carlos III de Madrid, C/ Madrid 126, 28903 Getafe (Madrid), e-mail: juan.romo@uc3m.es

1 Introduction

Classification of time series is a statistical matter with many applications. Time series can be studied from both time and frequency domains; while the former uses position or time as index, the latter involves the frequency. With short stationary series the usual multivariate techniques can be applied as a time domain approach, but a frequency domain approach is more appropriate with long series because of the dimensional reduction it implies, and this domain is particularly important for nonstationary series (Huang et al. [2004]). There are many works on classification methods for stationary processes in both domains (see references in chapter 7 of Taniguchi and Kakizawa [2000]). On the other hand, several authors have dealt with the discrimination between nonstationary models: Hastie et al. (1995), Shumway (2003), Huang et al. (2004), Hirukawa (2004), Sakiyama and Taniguchi (2004), Chandler and Polonik (2006) and Maharaj and Alonso (2007), among others. Our procedure must be considered in the frequency domain.

Since the integrated periodogram can be seen as a function, we shall use specific techniques for functional data. Nowadays functional data are present in many areas, sometimes because they are the output of measurement processes, other times for theoretical or practical reasons. There are several works on the statistical analysis of functional data and, particularly, on their classification. For example, a penalized discriminant analysis is proposed in Hastie et al. (1995); it is adequate for situations with many highly correlated predictors, as those obtained by discretizing a function. Nonparametric tools to classify a set of curves have been introduced in Ferraty and Vieu (2003), where authors calculate the posterior probability of belonging to a given class of functions by using a consistent kernel estimator. A new method for extending classical linear discriminant analysis to functional data has been analysed in James and Hastie (2001); this technique is particularly useful when only fragments of the curves are observed. The problem of unsupervised classification or clustering of curves is addressed in James and Sugar (2003), who elaborate a flexible model--based approach for clustering functional data; it is effective when the observations are sparse, irregularly spaced or occur at different time points for each subject. In Abraham et al. (2003) unsupervised clustering of functions is considered; they fit the data by B-splines and partition is done over the estimated model coefficients using a k-means algorithm. In a related problem, Hall et al. (2001) explore a functional data-analytic approach to perform signal discrimination. Nevertheless, many of these procedures are highly sensitive to outliers. A simple idea to classify functions is to minimize the distance between the new curve and a reference one of the group. The approach presented in this paper follows this idea. As a reference function of each group we shall take the mean of the integrated periodograms of its elements. Later this curve will be substituted for a more robust representative.

The notion of statistical *depth* has been extended to functional data, and López-Pintado and Romo (2006) have used this concept to classify curves. As these authors write, *a statistical depth expresses the "centrality" or "outlyingness" of an observation within a set of data (or with respect*

to a probability distribution) and provides a criterion to order observations from center-outward. Since robustness is an interesting feature of the statistical methods based on depth, we have applied the ideas of López-Pintado and Romo (2008) to add robustness to our time series classification procedure. Their method considers the α-trimmed mean as a reference curve of each group, which is defined as the average of the $1-\alpha$ proportion of the deepest curves of the sample; that is, it leaves $100\alpha\%$ of data out. This trim is the responsible for adding robustness.

Next sections are organized as follows. In section 2 we include some definitions and describe the classification algorithm. In section 3 we explain how depth can be used to make the method robust. Next two sections, 4 and 5, show the behavior of the procedure with simulated and real data, respectively. A brief summary of conclusions is given in section 6.

2 Classification Method

One of the main points of our classification proposal is that we turn the time series problem in a functional data problem by considering the integrated periodogram of each time series. Then we can use the statistical inference of this kind of data: concepts, definitions, procedures, etcetera.

The Fourier transform of the correlation function of a process, when it is absolutely summable, is known as *spectral density* or *spectrum*; its integration provides the *spectral distribution function* or *cumulative spectrum*. Let X_t be a stationary process with autocovariance function $\gamma(h) = cov(X_t, X_{t-h})$ satisfying $\sum_{h=-\infty}^{+\infty} |\gamma(h)| < +\infty$, then the spectral density is expressed as $f(\omega) = \sum_{h=-\infty}^{+\infty} \gamma(h) \exp(-2\pi i h\omega)$, and it holds that $\gamma(h) = \int_{-1/2}^{+1/2} \exp(2\pi i h\omega) dF(\omega)$, where F is the spectral distribution function.

The *periodogram* is the sample version of the population concept of spectral density, and it expresses the contribution of the frequencies to the variance of a series. Let $X = (x_1, \ldots, x_T)$ be a time series, the periodogram is obtained by:

$$I_T(\omega_k) = \sum_{h=-(T-1)}^{+(T-1)} \hat{\gamma}(h) \exp(-2\pi i h\omega_k), \tag{1}$$

with ω_k taking values in $\{k/T \mid k = 0, \ldots, [T/2]\}$, the discrete *Fourier frequencies* set.

Its cumulative version is the *integrated periodogram*, $F_T(\omega_k) = \sum_{i=1}^{k} I_T(\omega_i)$, also named *cumulative periodogram*; or with a normalization:

$$F_T(\omega_k) = \sum_{i=1}^{k} I_T(\omega_i) / \sum_{i=1}^{m} I_T(\omega_i), \tag{2}$$

where m is the cardinal of the Fourier frequencies set. The normalized version of the cumulative periodogram puts emphasis on the shape of the curves, not on the scale, as the nonnormalized version does. In our case, since depth is not highly dependent on shape, a simple criterion we propose is using the former when the graphs of the functions of the different groups tend to intersect and using the latter when the graphs do not tend to intersect. In that case normalization

dissolves the confusing area caused by the intersections. In general, among other advantages of the integrated periodogram are: it is nondecreasing and quite smooth curve (the integration is a sort of smoothing); it has good asymptotic properties (while the periodogram is an asymptotically unbiased but inconsistent estimator of the spectral density, the integrated periodogram is a consistent estimator of the spectral distribution); although in practice for stationary processes the integrated spectrum is usually estimated via the estimation of the spectrum, from the theoretical point of view the spectral distribution always exists and only when it is absolutely continuous the spectral density exists; finally, theoretically the integrated spectrum determines completely the stochastic processes.

Previous definitions, (1) and (2), are limited to some discrete values of the frequency ω, but they can be extended to any value in the interval $(-1/2, +1/2)$. Apart from anything else the periodogram is defined only for stationary series, but in order to be able to classify nonstationary time series we shall consider that series are locally stationary. With this assumption we shall be allowed to split them into blocks, compute the integrated periodogram of each block and merge these periodograms in a final curve; that is, the idea is to approximate the locally stationary processes by piecewise stationary processes. In figure 1(b) we illustrate our blockwise spectral distribution estimation of the locally stationary process spectrum. It is worth mentioning that there are two opposite effects as a consequence of splitting: one is that the narrower blocks are, the closer to the locally stationarity assumption we are; the other is that when the length of blocks decreases, also decreases the quality of the integrated periodogram as estimator of the integrated spectrum.

When functions—instead of time series—need to be classified, a possible criterion is to assign them to the group minimizing some distance from the new data to the group. In our context this criterion means that we classify new series in the group minimizing the distance between the integrated periodogram of the series and a reference curve. As a reference function of each group we take the mean of its elements, as it summarizes the general behaviour of the sample. Let $\Psi_{g_i}(\omega)$; $i = 1, \ldots, N$ be functions of group g, the mean is defined as:

$$\bar{\Psi}_g = \frac{1}{N} \sum_{i=1}^{N} \Psi_{g_i}(\omega). \tag{3}$$

In our case, $\Psi_{g_i}(\omega)$ is the joint of the integrated periodograms of the blocks for the i-th series in group g.

As a distance measurement between two functions we have taken the L_1 distance that, for the functions $\Psi_1(\omega)$ and $\Psi_2(\omega)$, is defined as:

$$d(\Psi_1, \Psi_2) = \int_{-1/2}^{+1/2} |\Psi_1(\omega) - \Psi_2(\omega)| d\omega. \tag{4}$$

Notice that the functions we are working with, that is, the integrated periodograms, belong to the $L_1[-1/2, +1/2]$ space. Some other distance could be considered, since in general there is not

"the best" one. For example, with the L_2 distance big differences between functions would be highlighted and so would be the corresponding values of the independent variable (frecuency).

With these definitions, we can enunciate the classification algorithm:

Algorithm 1

Let $\{X_1, \ldots, X_{N_x}\}$ be a sample containing N_x time series from the population P_X, and let $\{Y_1, \ldots, Y_{N_y}\}$ be a sample containing N_y series from P_Y. The classification method comprises the following steps:

1. To obtain the functional data, the associate curve of each time series is constructed by merging the integrated periodograms of the k blocks into which series are split: $\{\Psi_{X_1}, \ldots, \Psi_{X_{N_x}}\}$ and $\{\Psi_{Y_1}, \ldots, \Psi_{Y_{N_y}}\}$, where $\Psi_{X_i} = (F_{X_i}^{(1)} \ldots F_{X_i}^{(k)})$, $\Psi_{Y_i} = (F_{Y_i}^{(1)} \ldots F_{Y_i}^{(k)})$ and $F_{X_i}^{(j)}$ is the integrated periodogram of the j-th block of the i-th series of the population X; for the population Y notation $F_{Y_i}^{(j)}$ has the equivalent meaning.
2. For both P_X and P_Y populations the group mean of these functions is calculated: $\bar{\Psi}_X$ and $\bar{\Psi}_Y$.
3. Let Ψ_Z be the associate curve of a new series Z, that is $\Psi_Z = (F_Z^{(1)} \ldots F_Z^{(k)})$, then Z is classified in the group P_X if $d(\Psi_Z, \bar{\Psi}_X) < d(\Psi_Z, \bar{\Psi}_Y)$, and in the group P_Y otherwise.

Remark 1: To apply the algorithm to stationary series k can be set equal to 1. We have used a dyadic splitting of the series into blocks in the simulation and real data computations, that is, $k = 2^p, p = 0, 1, \ldots$; but the implementation with blocks of different lengths, as it could be suggested by visual inspection of data, is also possible.

Remark 2: Though we are considering $G = 2$ in this paper, the classification method is obviously extended to the general case in which there are G different groups or populations, P_g, with $g = 1, \ldots, G$.

Remark 3: The same methodology that we propose in this paper could be implemented using some different classification criterion between curves, reference function —or functions— of each group (as we do in the following section) and distance between curves.

3 Robust Version

Our classification method depends on the group reference curve to which the distance is measured. The mean of a set of functions is not robust to the presence of outliers. Then robustness can be

added to the classification procedure by using a robust reference curve. Instead of considering the mean of the integrated periodograms of all the elements of the group, we shall consider the α-trimmed mean, where only the deepest elements are averaged. The trim adds robustness by making the reference curve more resistant to the presence of outliers. In this section we describe the concept of depth extended to functional data by López-Pintado and Romo (2008). Then we propose a robust version of our classification algorithm.

The statistical concept of *depth* is a measurement of the "centrality" of each element inside the sample. This means, for example, that in a set of points of $\mathbb{R}^n$ the closer to the mass center a point is, the deepest it is. The same general idea applies to other type of data, including functions. Different definitions of depth for functions can be given.

Let $G(\Psi) = \{(t, \Psi(t)) \mid t \in [a, b]\}$ denote the graph in $\mathbb{R}^2$ of a function $\Psi \in C[a, b]$. Let $\Psi_i(t)$, $i = 1, \ldots, N$, be functions in $C[a, b]$, then a subset of this functions, $\Psi_{i_j}(t)$, $j = 1, \ldots, k$, determines a band in $\mathbb{R}^2$

$$B(\Psi_{i_1}, \ldots, \Psi_{i_k}) = \{(t, y) \mid t \in [a, b], \min_{r=1,\ldots,k} \Psi_{i_r}(t) \leq y \leq \max_{r=1,\ldots,k} \Psi_{i_r}(t)\}. \tag{5}$$

For any of the functions Ψ, the quantity

$$BD_N^{(j)}(\Psi) = \binom{N}{j}^{-1} \sum_{1 \leq i_1 < i_2 < \ldots < i_j \leq N} I\{G(\Psi) \subset V(\Psi_{i_1}, \ldots, \Psi_{i_j})\}, \qquad j \geq 2 \tag{6}$$

expresses the proportion of bands, determined by j different curves, $\Psi_{i_1}, \ldots, \Psi_{i_j}$, containing the graph of Ψ (the indicator function takes the value $I\{A\} = 1$ if A occurs, and $I\{A\} = 0$ otherwise). The definition of depth for functional data introduced by López-Pintado and Romo (2008) states that for functions $\Psi_i(t)$, $i = 1, \ldots, N$, the *band depth* of any of these curves Ψ is

$$BD_{N,J}(\Psi) = \sum_{j=2}^{J} BD_N^{(j)}(\Psi), \qquad 2 \leq J \leq N. \tag{7}$$

If $\tilde{\Psi}$ is the stochastic process that has generated the observations $\Psi_i(t)$, $i = 1, \ldots, N$, the population versions of these indexes are $BD^{(j)}(\Psi) = P\{G(\Psi) \subset B(\tilde{\Psi}_{i_1}, \ldots, \tilde{\Psi}_{i_j})\}$, $j \geq 2$, and $BD_J(\Psi) = \sum_{j=2}^{J} S^{(j} = \sum_{j=2}^{J} P\{G(\Psi) \subset B(\tilde{\Psi}_{i_1}, \ldots, \tilde{\Psi}_{i_j})\}$, $J \geq 2$, respectively.

A more flexible notion of depth is also defined in López-Pintado and Romo (2008): the *modified band depth*. The indicator function in definition (6) is replaced by the length of the set where the function is inside the corresponding band. For any function Ψ of $\Psi_t(t)$, $i = 1, \ldots, N$, and $2 \leq \ j \geq N$, let

$$A_j(\Psi) \equiv A(\Psi; \Psi_{i_1}, \ldots, \Psi_{i_j}) \equiv \{t \in [a, b] \mid \min_{r=i_1,\ldots,i_j} \Psi_r(t) \leq \Psi(t) \leq \max_{r=i_1,\ldots,i_j} \Psi_r(t)\}. \tag{8}$$

be the set of points in the interval $[a, b]$ where the function Ψ is inside the band. If λ is the Lebesgue measure on the interval $[a, b]$, $\lambda(A_j(\Psi))$ is the "proportion of time" that Ψ is inside the band. Then,

$$MBD_N^{(j)}(\Psi) = \binom{N}{j}^{-1} \lambda([a, b])^{-1} \sum_{1 \leq i_1 < i_2 < \ldots < i_j \leq N} \lambda(A(\Psi; \Psi_{i_1}, \ldots, \Psi_{i_j})), \qquad 2 \leq j \leq N, \tag{9}$$

is the generalized version of $BD_N^{(j)}$. If Ψ is always inside the band, the measure $\lambda(A_j(\Psi))$ is 1 and this generalizes the definition of depth given in (7). Finally, the generalized band depth of any of the curves Ψ in $\Psi_i(t)$, $i = 1, \ldots, N$, is

$$MBD_{N,J}(\Psi) = \sum_{j=2}^{J} MBD_N^{(j)}(\Psi), \qquad 2 \leq J \leq N. \tag{10}$$

If $\tilde{\Psi}_i(t)$, $i = 1, \ldots, N$, are independent copies of the stochastic process $\tilde{\Psi}$ which generates the observations $\Psi_i(t)$, $i = 1, \ldots, N$, the population versions of these depth indexes are, respectively, $MBD^{(j)}(\Psi) = \mathbb{E}\lambda(A(\Psi; \tilde{\Psi}_{i_1}, \ldots, \tilde{\Psi}_{i_j}))$, $2 \leq J \geq N$, and $MBD_J(\Psi) = \sum_{j=2}^{J} MBD^{(j)}(\Psi) = \sum_{j=2}^{J} \mathbb{E}\lambda(A(\Psi; \tilde{\Psi}_{i_1}, \ldots, \tilde{\Psi}_{i_j}))$, $2 \leq J \leq N$. We have used the value $J = 2$, since the modified band depth is very stable in J, providing similar center-outward order in a collection of functions (López-Pintado and Romo [2006, 2008]).

In order to add robustness to the algorithm presented in the previous section, now we take the group α-trimmed mean of its elements as the reference function. Let $\Psi_{g_{(i)}}(t)$, $i = 1, \ldots, N$, be functions of the class g ordered by decreasing depth, the α-trimmed mean is defined as:

$$\bar{\Psi}_g^{\alpha} = \frac{1}{N - [N\alpha]} \sum_{i=1}^{N-[N\alpha]} \Psi_{g_{(i)}}(t), \tag{11}$$

where $[\cdot]$ is the integer part function. Notice that the median (in the sense of "the deepest") function is also included in the previous expression; nevertheless, the α-trimmed mean is robust either, as the median, and summarizes the general behaviour of the functions, as the mean. In our simulation and real data exercises, a value of $\alpha = 0.2$ is used. It means that for each group the 20% of the less depth data are leaved out. This is the value used in López-Pintado and Romo (2006).

With this little—but essential—difference the algorithm hardly changes. At step 2 the group α-trimmed mean is taken instead of the group mean, that is, now the distance from the series to the class is measured from a different reference curve of the class.

Algorithm 2

Let $\{X_1, \ldots, X_{N_x}\}$ be a sample containing time series from the population P_X, and let $\{Y_1, \ldots, Y_{N_y}\}$ be a sample from P_Y. The classification method comprises the following steps:

1. To obtain the functional data, the associate curve of each time series is constructed by merging the integrated periodograms of the k blocks into which series are split: $\{\Psi_{X_1}, \ldots, \Psi_{X_{N_x}}\}$ and $\{\Psi_{Y_1}, \ldots, \Psi_{Y_{N_y}}\}$, where $\Psi_{X_i} = (F_{X_i}^{(1)} \ldots F_{X_i}^{(k)})$, $\Psi_{Y_i} = (F_{Y_i}^{(1)} \ldots F_{Y_i}^{(k)})$ and $F_{X_i}^{(j)}$ is the integrated periodogram of the j-th block of the i-th series of the population X; for the population Y notation $F_{Y_i}^{(j)}$ has the equivalent meaning.

2. For both P_X and P_Y populations the α-trimmed group mean of these functions is computed: $\bar{\Psi}_X^\alpha$ and $\bar{\Psi}_Y^\alpha$.
3. Let Ψ_Z be the associate curve of a new series Z, that is $\Psi_Z = (F_Z^{(1)} \dots F_Z^{(k)})$, then Z is classified in the group P_X if $d(\Psi_Z, \bar{\Psi}_X^\alpha) < d(\Psi_Z, \bar{\Psi}_Y^\alpha)$, and in the group P_Y otherwise.

Remark 4: The same algorithm could be implemented using a different functional depth.

4 Simulations

In the simulation studies we evaluate our two algorithms and, as a reference, the method proposed in Huang et al. (2004). The results obtained with algorithm 1 are denoted by DbC, the results with algorithm 2 by DbC-α and the method of Huang et al. (2004) by SLEXbC. Ombao et al. (2001) introduced the SLEX (smooth localized complex exponentials) model of a nonstationary random process, and the method of Huang et al. (2004) uses SLEX, a set of Fourier-type bases that are at the same time orthogonal and localized in both time and frequency domains. In a first step, they select from SLEX a basis explaining as good as possible the difference between the classes of time series. After this they construct a discriminant criterion that is related to the SLEX spectra of the different classes: a time series is assigned to the class minimizing the Kullback-Leibler divergence between the estimated spectrum and the spectrum of the class. For the SLEXbC method we have used an implementation provided by the authors (see `http://www.stat.uiuc.edu/õmbao/research.html`). To select the parameters for this method, we have done a small optimization for each simulation exercise and the results were similar to the values recommended to us by the authors.

We have used the same models than Huang et al. (2004). For each comparison of two classes, we run 1000 times the following steps. We generate training and test sets of each model/class. Training sets have the same sizes (sample size and series length) they used, and test sets contain always 10 series of the length involved in each particular simulation exercise. Then the methods are called with exactly the same data sets; that is, in these models exactly the same simulated time series are used by the three methods, including the calls to our algorithms with different values of k.

Simulation Exercise 1: We compare an autoregressive process of order one (X_t) with Gaussian white noise (Y_t):

$$\begin{aligned} X_t^{(i)} &= \phi \cdot X_{t-1}^{(i)} + \epsilon_t^{(i)} \qquad t = 1, \dots, T_x \text{ and } i = 1, \dots, N_x \\ Y_t^{(j)} &= \epsilon_t^{(j)} \qquad\qquad\qquad t = 1, \dots, T_y \text{ and } j = 1, \dots, N_y, \end{aligned} \tag{12}$$

where $\epsilon_t^{(i)}$ y $\epsilon_t^{(j)}$ are i.i.d. $N(0,1)$. Each training data set has $N_x = N_y = 8$ series of length $T_x = T_y = 1024$. Six comparisons have been run, with the parameter ϕ of the AR(1) model taking the values -0.5, -0.3, -0.1, $+0.1$, $+0.3$ and $+0.5$. Series are stationary in this exercise.

Simulation Exercise 2: We compare two processes composed half by white noise and half by an autoregressive process of order one. The value of the AR(1) parameter is -0.1 in the first class and $+0.1$ in the second class:

$$X_t^{(i)} = \begin{cases} \epsilon_t^{(i)} & \text{if } t = 1, \ldots, T_x/2 \\ X_t^{(i)} = -0.1 \cdot X_{t-1}^{(i)} + \epsilon_t^{(i)} & \text{if } t = T_x/2+1, \ldots, T_x \end{cases}$$
$$Y_t^{(j)} = \begin{cases} \epsilon_t^{(j)} & \text{if } t = 1, \ldots, T_y/2 \\ Y_t^{(j)} = +0.1 \cdot Y_{t-1}^{(j)} + \epsilon_t^{(j)} & \text{if } t = T_y/2+1, \ldots, T_y \end{cases} \tag{13}$$

with $i = 1, \ldots, N_x$ and $j = 1, \ldots, N_y$. Different combinations of training sample sizes —$N_x = N_y = 8$ and 16— and series lengths —$T_x = T_y = 512$, 1024 and 2048— are considered. In this exercise series are composed of stationary parts (they are piecewise stationary series), but series themselves are not.

Simulation Exercise 3: In this exercise the stochastic models of both classes are slowly time-varying second order autoregressive processes:

$$\begin{aligned} X_t^{(i)} &= a_{t;0.5} \cdot X_{t-1}^{(i)} - 0.81 \cdot X_{t-2}^{(i)} + \epsilon_t^{(i)} \qquad t = 1, \ldots, T_x \\ Y_t^{(j)} &= a_{t;\tau} \cdot Y_{t-1}^{(j)} - 0.81 \cdot Y_{t-2}^{(j)} + \epsilon_t^{(j)} \qquad t = 1, \ldots, T_y \end{aligned} \tag{14}$$

with $i = 1, \ldots, N_x$, $j = 1, \ldots, N_y$ and $a_{t;\tau} = 0.8 \cdot [1 - \tau \cos(\pi t/1024)]$, where τ is a parameter. Each training data set has $N_x = N_y = 10$ series of length $T_x = T_y = 1024$. Three comparisons have been done, the first class having always the parameter $\tau = 0.5$, and the second class having respectively the values $\tau = 0.4$, 0.3 and 0.2. Notice that a coefficient of the autoregressive structure is not fixed but it varies in time; this cause that the processes are not stationary. See figure 1(a) for an example of the integrated spectrum corresponding to these processes.

We have tested that the values between $\tau = -0.9$ and $\tau = +0.9$ do not produce that, for some value of t, the characteristic polynomial of the autoregressive process had roots inside the unit circle.

In order to test the robustness of our procedure and the SLEXbC procedure, we perform additional experiments where the training set is contaminated with an outlier time series. In all

Figure 1: Time-varying autoregressive model with $\tau = 0.4$

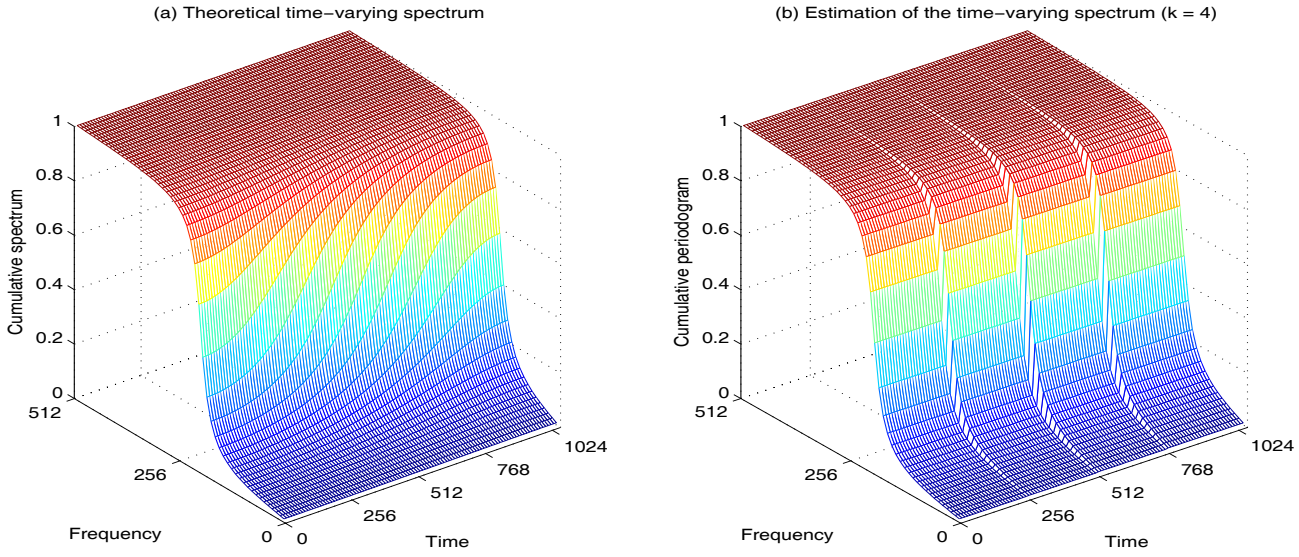

cases we contaminate the P_X population by changing one series for another following a different model. We consider three levels of contamination: one type of weak contamination (A) and two strong contaminations (B and C).

Contamination A: For exercise 1 it consists in substituting the autoregressive structure for a moving average structure; that is, generating a MA(1) model —with the MA parameter equal to the AR parameter— instead of a AR(1) model. For exercise 2 it consists in doing the same substitution of structures, but now only in the autoregressive half of one series of a class (the other half is white noise). For exercise 3 we contaminate the set of slowly time-varying autoregressives of parameter +0.5 with a series of the same model but with parameter value +0.2.

Contamination B: This contamination consists in using a parameter value of $\phi = -0.9$, in exercises 1 and 2, and $\tau = -0.9$, in exercise 3, instead of the correct value. That is, it consists in using always the correct model but mistaking the parameter value in a series.

Contamination C: Equal to the contamination B but using a value +0.9, instead of -0.9.

In figures 2(a) and 2(b) we illustrate the three contaminations for the first two exercises with specific parameter values. Figure 2(c) shows the contamination B for the third exercise.

The error rates estimates for the first simulation experiment are presented in table 1; for the second simulation experiment in tables 2, 3, 4 and 5; and for the third simulation experiment in

Figure 2: Examples of contaminations for the three simulation experiments

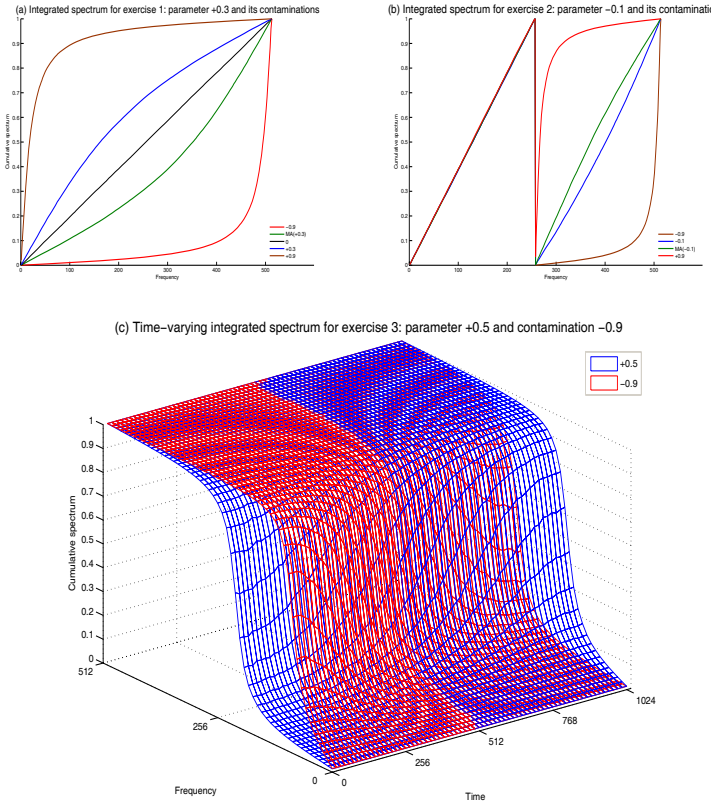

tables 6, 7, 8 and 9. Each cell includes the mean and the standard error (in parenthesis) of the 1000 runs.

Tables 10, 11 and 12 provide the estimates of the computation times. In these tables each cell includes the mean of the 1000 runs, in seconds. For each method this time is measured just from the instant when the series are inputted to the method to the moment when the method outputs the error rate. This means that training and test series generation time is not included in the computation; but for our method the computation does include the construction of functional data from series and the evaluation of depth inside groups. Simulation exercises have been run on a personal computer with the following processor and RAM memory: AMD Athlon(tm) 64 Processor 3200+ 2.01GHz, 2.00Gb RAM.

For all tables we use the following notation: DbC (from *depth-based classification*) for algorithm 1, DbC-α for algorithm 2 and SLEXbC for the method of Huang et al. (2004). When a number follows DbC or DbC-α, it is the value of k, that is, the number of blocks into which the series are split. The digits in bold correspond to the minima (when they are different to zero).

Comments on error rates

Table 1 shows the estimates of the misclassification rates for the first simulation exercise. We

Table 1: Misclassification rates estimates for simulation exercise 1 with and without contamination

	$\phi =$ **-0.5**	$\phi =$ **-0.3**	$\phi =$ **-0.1**	$\phi =$ **+0.1**	$\phi =$ **+0.3**	$\phi =$ **+0.5**
Without contamination						
DbC	0.000 (0.0000)	0.000 (0.0000)	**0.063** (0.0017)	**0.060** (0.0017)	0.000 (0.0000)	0.000 (0.0000)
DbC-α	0.000 (0.0000)	0.000 (0.0000)	0.065 (0.0018)	0.062 (0.0017)	0.000 (0.0000)	0.000 (0.0000)
SLEXbC	0.000 (0.0000)	0.000 (0.0000)	0.131 (0.0024)	0.127 (0.0024)	0.000 (0.0000)	0.000 (0.0000)
Contamination A						
DbC	0.000 (0.0000)	0.000 (0.0001)	0.077 (0.0019)	0.074 (0.0019)	0.000 (0.0001)	0.000 (0.0000)
DbC-α	0.000 (0.0000)	**0.000** (0.0000)	**0.064** (0.0017)	**0.062** (0.0017)	**0.000** (0.0000)	0.000 (0.0000)
SLEXbC	0.000 (0.0000)	0.000 (0.0001)	0.175 (0.0028)	0.172 (0.0029)	0.000 (0.0001)	0.000 (0.0000)
Contamination B						
DbC	0.000 (0.0000)	0.000 (0.0001)	0.300 (0.0028)	0.513 (0.0012)	0.001 (0.0002)	0.000 (0.0000)
DbC-α	0.000 (0.0000)	**0.000** (0.0000)	**0.065** (0.0018)	**0.062** (0.0017)	**0.000** (0.0000)	0.000 (0.0000)
SLEXbC	0.000 (0.0000)	0.001 (0.0002)	0.377 (0.0025)	0.491 (0.0011)	0.002 (0.0003)	0.000 (0.0000)
Contamination C						
DbC	0.000 (0.0000)	0.001 (0.0002)	0.512 (0.0013)	0.300 (0.0027)	0.000 (0.0001)	0.000 (0.0000)
DbC-α	0.000 (0.0000)	**0.000** (0.0000)	**0.064** (0.0017)	**0.062** (0.0017)	**0.000** (0.0000)	0.000 (0.0000)
SLEXbC	0.000 (0.0000)	0.002 (0.0004)	0.490 (0.0011)	0.377 (0.0025)	0.001 (0.0002)	0.000 (0.0000)

can observe that when contamination is not present DbC and DbC-α provide similar error rates, and about half of the ones obtaining by SLEXbC. As we could expect, for DbC and SLEXbC error rates increase slightly with contamination A (weak) and notably with contaminations B and C (strong), while changes are negligible for DbC-α because the trim keeps the contamination out. DbC has an error about half of SLEXbC for contamination A, but their errors are similar with contaminations B and C. The three methods have no misclassifications for series easy to assign, that is, for values of ϕ far from 0 (the value for the Gaussian white noise). There are some symmetries in table 1 for DbC and SLEXbC: for example, contamination with $\phi = -0.9$ has similar effect on models with ϕ negative/positive than contamination with $\phi = +0.9$ has on models with parameter positive/negative, respectively. To complement the information provided by the tables (mean and standard error), we include some boxplots of the misclassification rates estimates. For exercise 1 we include only the plot of one of the two most difficult comparison, that is, the comparisons of models $\phi = +0.1$ with Gaussian white noise (see figure 3). The plot shows that SLEXbC tends to have higher median, higher errors above this median, and less errors near zero. On the other side, DbC-α is the only method maintaining the same pattern (with and without contamination) and a considerable amount of errors close to zero.

Figure 3: Boxplot of the misclassification rates in the simulation exercise 1, parameters values +0.1 versus 0

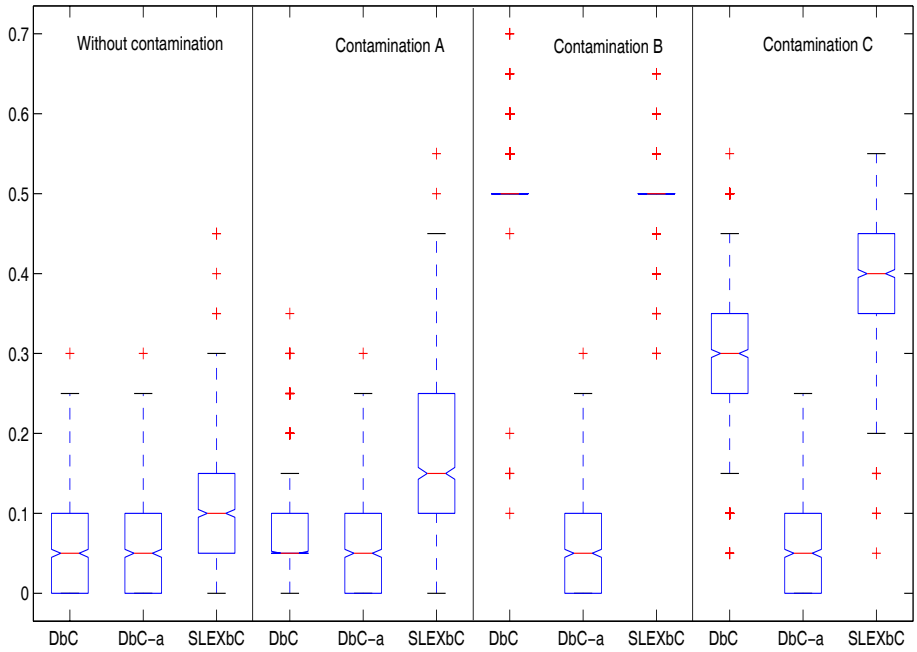

Tables 2, 3, 4 and 5 provide the results of the second simulation exercise. As we could expect, errors decrease when any parameter, N or T, increases. Our methods obtain the minimum errors when series are divided into two blocks. While our errors are bigger than errors of SLEXbC when we consider the whole series (without splitting them into blocks), errors fall with the first division. As we mentioned, the length of the blocks decreases with k, and either decreases the quality of the periodogram as estimator. We can also observe this effect of splitting in all the tables of simulation exercise 2, and it is also evident that the increase in errors with the increase of k is higher for short series than for longer ones. Let us remind that, like our procedure, the SLEXbC method splits implicitly the series into blocks. Respecting the contaminations, for DbC and SLEXbC errors increase slightly with contamination A and greatly for contaminations B and C, while DbC-α maintains its errors and performs the best, mainly with strong contaminations, when two blocks are considered. As it could be expected, contaminating a series has major effects when samples sizes are $N_x = N_y = 8$ than when $N_x = N_y = 16$. The DbC and SLEXbC methods are affected more for contamination C than for contamination B, since $\phi = +0.9$ is farther from $\phi = -0.1$ (population P_X) than $\phi = -0.9$ is.

Concerning the boxplots in exercise 2, again DbC and DbC-α perform better than SLEXbC, and in the plot (see figure 4) it can be noticed that when $k > 1$ the median error rate decreases and it presents a stable behaviour. These plots, like tables, show that DbC-α with $k = 2$ tends to provide the best results, except when there is no contamination, when DbC with $k = 2$ has the best performance. In general, DbC-α with $k = 2$ is the method that presents the biggest

Table 2: Misclassification rates estimates for simulation exercise 2 without contamination

	NxT = **8x512**	**16x512**	**8x1024**	**16x1024**	**8x2048**	**16x2048**
DbC 1	0.141 (0.0024)	0.131 (0.0024)	0.062 (0.0017)	0.060 (0.0017)	0.014 (0.0008)	0.014 (0.0008)
2	**0.066** (0.0017)	**0.061** (0.0017)	**0.015** (0.0009)	**0.014** (0.0008)	**0.001** (0.0003)	**0.001** (0.0003)
4	0.078 (0.0019)	0.069 (0.0018)	**0.015** (0.0009)	0.014 (0.0009)	**0.001** (0.0003)	**0.001** (0.0003)
8	0.090 (0.0020)	0.080 (0.0019)	0.020 (0.0010)	0.018 (0.0009)	0.002 (0.0003)	**0.001** (0.0003)
DbC-α 1	0.143 (0.0024)	0.132 (0.0024)	0.063 (0.0017)	0.061 (0.0017)	0.015 (0.0009)	0.014 (0.0008)
2	0.069 (0.0018)	0.064 (0.0017)	0.016 (0.0009)	0.015 (0.0009)	**0.001** (0.0003)	**0.001** (0.0003)
4	0.083 (0.0020)	0.073 (0.0018)	0.017 (0.0010)	0.016 (0.0009)	0.002 (0.0003)	**0.001** (0.0003)
8	0.105 (0.0023)	0.088 (0.0020)	0.024 (0.0011)	0.019 (0.0010)	0.002 (0.0004)	0.002 (0.0003)
SLEXbC	0.114 (0.0023)	0.086 (0.0020)	0.038 (0.0014)	0.025 (0.0011)	0.007 (0.0006)	0.003 (0.0004)

proportion of errors near zero.

For simulation exercise 3, conclusions similar to the previous can be derived from tables 6, 7, 8 and 9. They show also that in our proposal penalization for splitting too much is not serious when series are long enough. With the presence of contamination, the best errors are obtained by DbC-α for $k = 4$. As we can see, contamination A has slight effect. On the other side, results are very different for contaminations B and C. Notice that as τ has positive values in both populations, contaminating with a series of parameter $\tau = -0.9$ (contamination B) is a stronger contamination than using a series with $\tau = +0.9$ (contamination C).

Finally, in the three experiments a subtle effect can be seen between DbC and DbC-α. When there is no contamination it is normal for the former to provide slightly better error rates, because the latter, due to its trim, is using only $100(1 - \alpha)\%$ of the suitable training data available.

Comments on computation times

Estimates of the computation times are given in tables 10, 11 and 12. The computation time depends on the implementation —not just on the method itself—, so we pay closer attention to the qualitative interpretation of the results, as they are less dependent on the programmed code.

Since chronometer is called after generating series, it can be expected that the computation times not to depend on the parameters of the stochastic processes. This is what we observe for our algorithms, but not for the SLEXbC method. Perhaps this is because this method needs to select a basis of the SLEX library for each series, while our method works only with the graphs of the functions (and, at the same time, computing the integrated periodogram does not depend on the parameters).

Table 3: Misclassification rates estimates for simulation exercise 2 with contamination A

	NxT = 8x512	16x512	8x1024	16x1024	8x2048	16x2048
DbC 1	0.143 (0.0025)	0.132 (0.0024)	0.063 (0.0017)	0.062 (0.0017)	0.018 (0.0010)	0.015 (0.0008)
2	**0.070** (0.0018)	**0.062** (0.0017)	0.018 (0.0010)	**0.014** (0.0008)	0.002 (0.0003)	**0.001** (0.0003)
4	0.083 (0.0020)	0.071 (0.0019)	0.019 (0.0010)	0.015 (0.0009)	0.002 (0.0003)	**0.001** (0.0003)
8	0.102 (0.0022)	0.083 (0.0020)	0.026 (0.0012)	0.019 (0.0010)	0.003 (0.0004)	0.002 (0.0003)
DbC-α 1	0.145 (0.0025)	0.132 (0.0023)	0.063 (0.0017)	0.061 (0.0017)	0.015 (0.0009)	0.014 (0.0008)
2	0.072 (0.0018)	0.064 (0.0017)	**0.015** (0.0009)	0.015 (0.0009)	**0.001** (0.0002)	**0.001** (0.0003)
4	0.086 (0.0021)	0.073 (0.0018)	0.018 (0.0010)	0.016 (0.0009)	0.002 (0.0003)	**0.001** (0.0003)
8	0.114 (0.0024)	0.089 (0.0021)	0.025 (0.0011)	0.019 (0.0010)	0.003 (0.0004)	0.002 (0.0003)
SLEXbC	0.128 (0.0025)	0.092 (0.0021)	0.050 (0.0016)	0.027 (0.0012)	0.012 (0.0008)	0.004 (0.0004)

Table 4: Misclassification rates estimates for simulation exercise 2 with contamination B

	NxT = 8x512	16x512	8x1024	16x1024	8x2048	16x2048
DbC 1	0.258 (0.0029)	0.168 (0.0026)	0.252 (0.0029)	0.117 (0.0022)	0.250 (0.0029)	0.065 (0.0018)
2	0.135 (0.0024)	0.082 (0.0020)	0.088 (0.0021)	0.030 (0.0012)	0.049 (0.0016)	0.007 (0.0006)
4	0.137 (0.0025)	0.085 (0.0020)	0.089 (0.0021)	0.031 (0.0012)	0.049 (0.0016)	0.007 (0.0006)
8	0.143 (0.0025)	0.092 (0.0021)	0.093 (0.0022)	0.034 (0.0014)	0.050 (0.0016)	0.007 (0.0006)
DbC-α 1	0.145 (0.0024)	0.134 (0.0024)	0.064 (0.0017)	0.061 (0.0017)	0.015 (0.0008)	0.014 (0.0008)
2	**0.070** (0.0018)	**0.065** (0.0017)	**0.017** (0.0010)	**0.015** (0.0009)	0.003 (0.0006)	**0.001** (0.0003)
4	0.081 (0.0020)	0.071 (0.0019)	**0.017** (0.0010)	0.017 (0.0009)	**0.002** (0.0003)	0.002 (0.0003)
8	0.104 (0.0023)	0.087 (0.0020)	0.023 (0.0011)	0.019 (0.0010)	0.002 (0.0004)	0.002 (0.0003)
SLEXbC	0.239 (0.0031)	0.134 (0.0024)	0.228 (0.0030)	0.081 (0.0020)	0.220 (0.0030)	0.037 (0.0013)

Table 5: Misclassification rates estimates for simulation exercise 2 with contamination C

	NxT = **8x512**	**16x512**	**8x1024**	**16x1024**	**8x2048**	**16x2048**
DbC 1	0.457 (0.0056)	0.162 (0.0027)	0.437 (0.0055)	0.090 (0.0020)	0.445 (0.0047)	0.038 (0.0013)
2	0.147 (0.0036)	0.078 (0.0019)	0.055 (0.0020)	0.028 (0.0012)	0.015 (0.0010)	0.005 (0.0005)
4	0.187 (0.0037)	0.092 (0.0021)	0.068 (0.0022)	0.030 (0.0012)	0.017 (0.0010)	0.006 (0.0005)
8	0.225 (0.0039)	0.107 (0.0022)	0.101 (0.0027)	0.034 (0.0014)	0.024 (0.0011)	0.006 (0.0006)
DbC-α 1	0.145 (0.0025)	0.133 (0.0024)	0.063 (0.0017)	0.062 (0.0017)	0.015 (0.0009)	0.014 (0.0008)
2	**0.073** (0.0020)	**0.065** (0.0017)	0.018 (0.0013)	**0.015** (0.0009)	0.002 (0.0005)	**0.001** (0.0003)
4	0.083 (0.0020)	0.073 (0.0018)	**0.017** (0.0010)	0.016 (0.0009)	**0.002** (0.0003)	**0.001** (0.0003)
8	0.108 (0.0022)	0.088 (0.0021)	0.024 (0.0011)	0.019 (0.0010)	0.003 (0.0004)	0.002 (0.0003)
SLEXbC	0.376 (0.0036)	0.177 (0.0029)	0.354 (0.0032)	0.098 (0.0023)	0.369 (0.0030)	0.040 (0.0015)

Table 6: Misclassification rates estimates for simulation exercise 3 without contamination

	τ = **0.4**	τ = **0.3**	τ = **0.2**
DbC 1	0.218 (0.0031)	0.063 (0.0017)	0.019 (0.0010)
2	0.119 (0.0023)	0.006 (0.0006)	**0.000** (0.0000)
4	**0.101** (0.0022)	**0.002** (0.0003)	**0.000** (0.0000)
8	0.123 (0.0024)	0.003 (0.0004)	**0.000** (0.0000)
DbC-α 1	0.226 (0.0032)	0.065 (0.0018)	0.021 (0.0010)
2	0.128 (0.0023)	0.006 (0.0006)	**0.000** (0.0000)
4	0.112 (0.0023)	**0.002** (0.0003)	**0.000** (0.0000)
8	0.139 (0.0026)	0.004 (0.0004)	**0.000** (0.0000)
SLEXbC	0.181 (0.0031)	0.011 (0.0009)	**0.000** (0.0000)

Figure 4: Boxplots of the misclassification error rates for simulation exercise 2, training sets with 8 series of length 1024

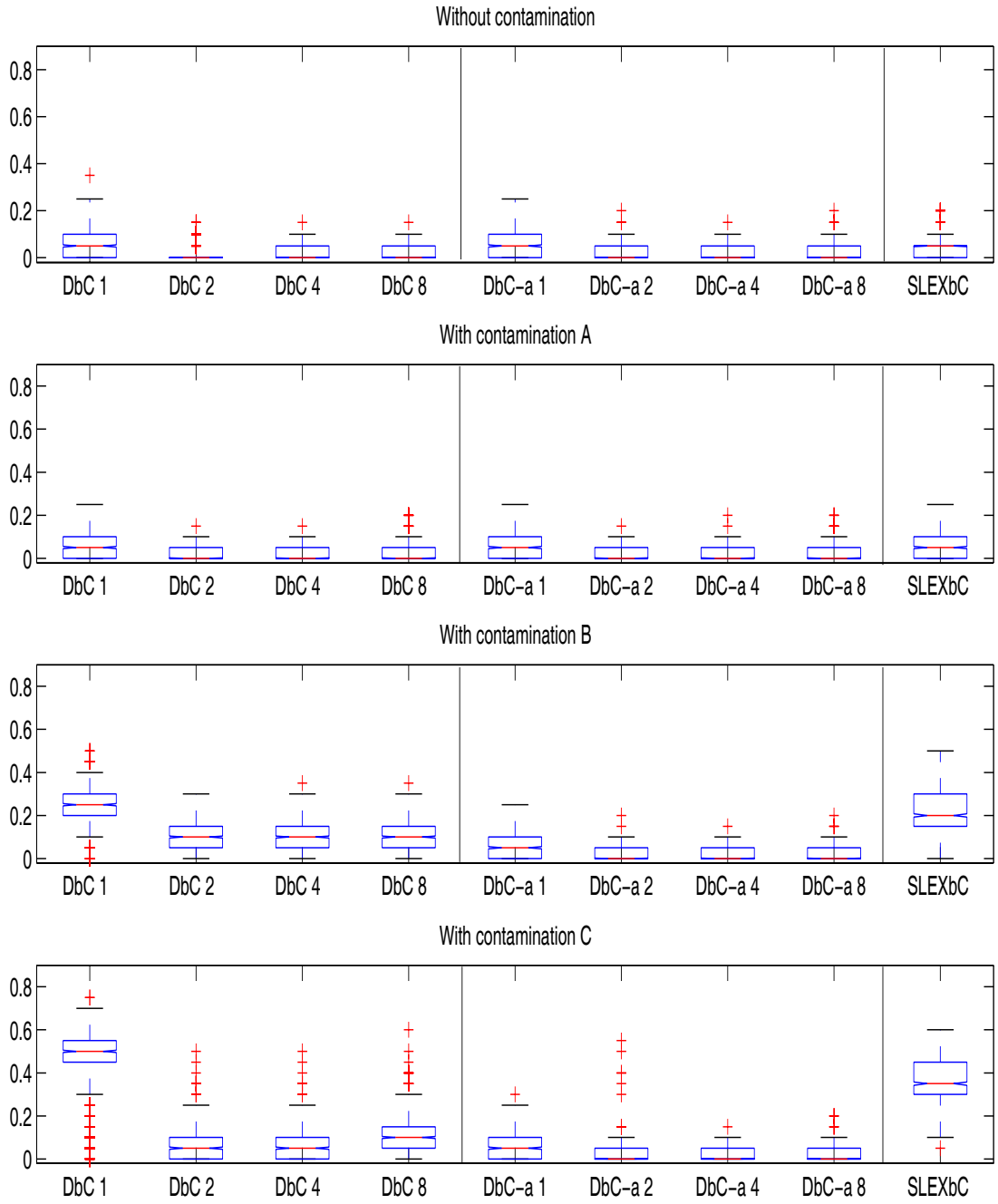

Table 7: Misclassification rates estimates for simulation exercise 3 with contamination A

	$\tau = \mathbf{0.4}$	$\tau = \mathbf{0.3}$	$\tau = \mathbf{0.2}$
DbC 1	0.232 (0.0032)	0.062 (0.0017)	0.019 (0.0009)
2	0.143 (0.0026)	0.006 (0.0006)	**0.000** (0.0000)
4	0.144 (0.0026)	0.004 (0.0004)	**0.000** (0.0000)
8	0.177 (0.0028)	0.005 (0.0005)	**0.000** (0.0000)
DbC-α 1	0.241 (0.0035)	0.065 (0.0018)	0.020 (0.0010)
2	0.131 (0.0025)	0.007 (0.0006)	**0.000** (0.0000)
4	**0.121** (0.0026)	**0.003** (0.0004)	**0.000** (0.0000)
8	0.150 (0.0029)	0.005 (0.0005)	**0.000** (0.0000)
SLEXbC	0.234 (0.0033)	0.016 (0.0011)	**0.000** (0.0000)

Table 8: Misclassification rates estimates for simulation exercise 3 with contamination B

	$\tau = \mathbf{0.4}$	$\tau = \mathbf{0.3}$	$\tau = \mathbf{0.2}$
DbC 1	0.254 (0.0029)	0.106 (0.0022)	0.043 (0.0015)
2	0.500 (0.0015)	0.067 (0.0021)	0.001 (0.0002)
4	0.500 (0.0012)	0.062 (0.0020)	0.001 (0.0002)
8	0.499 (0.0013)	0.082 (0.0024)	0.000 (0.0001)
DbC-α 1	0.231 (0.0031)	0.074 (0.0020)	0.026 (0.0012)
2	0.128 (0.0024)	0.007 (0.0006)	**0.000** (0.0000)
4	**0.113** (0.0023)	**0.002** (0.0004)	**0.000** (0.0000)
8	0.141 (0.0026)	0.003 (0.0004)	**0.000** (0.0000)
SLEXbC	0.492 (0.0019)	0.174 (0.0051)	0.015 (0.0009)

Table 9: Misclassification rates estimates for simulation exercise 3 with contamination C

	$\tau = \mathbf{0.4}$	$\tau = \mathbf{0.3}$	$\tau = \mathbf{0.2}$
DbC 1	0.257 (0.0029)	0.107 (0.0022)	0.044 (0.0015)
2	0.153 (0.0025)	0.017 (0.0009)	0.000 (0.0001)
4	0.128 (0.0024)	0.007 (0.0006)	**0.000** (0.0000)
8	0.132 (0.0024)	0.006 (0.0006)	0.000 (0.0001)
DbC-α 1	0.234 (0.0031)	0.074 (0.0020)	0.025 (0.0012)
2	0.125 (0.0024)	0.007 (0.0006)	0.000 (0.0001)
4	**0.114** (0.0024)	**0.002** (0.0004)	**0.000** (0.0000)
8	0.138 (0.0026)	0.004 (0.0004)	**0.000** (0.0000)
SLEXbC	0.173 (0.0027)	0.015 (0.0009)	0.000 (0.0001)

Table 10: Mean computation times for simulation exercise 1

	$\phi = \mathbf{-0.5}$	$\phi = \mathbf{-0.3}$	$\phi = \mathbf{-0.1}$	$\phi = \mathbf{+0.1}$	$\phi = \mathbf{+0.3}$	$\phi = \mathbf{+0.5}$
DbC	0.027	0.027	0.027	0.027	0.027	0.027
DbC-α	0.044	0.045	0.045	0.044	0.044	0.044
SLEXbC	0.632	0.678	0.724	0.713	0.670	0.619

Some other conclusions we can deduce from the three simulation exercises are the following. It is clear that for our procedure times increase with the number of blocks k. One can also see that the computation of depth is moderately time-consuming with the sample size and series length involved in exercises 1 and 3. This computation time should increase quite with sample size and a little with series length, since slowness cames from the number of comparisons the evaluation of depths includes, not for the time each of these comparisons takes. Nevertheless, it is possible to do these comparisons only once by implementing conveniently the method of López-Pintado and Romo (2006); such an implementation allows using their methods with bigger sample sizes. Finally, an interesting effect showed in table 11 is that computation time depends on sample size, N, for our approach, but it seems slightly dependent on the series length, T, while the SLEXbC method gets slower when any N or T increases.

5 Real Data

We have evaluated our proposal in a benchmark data set containing eight explosions, eight earthquakes and one extra series —known as NZ event— not classified (but being an earthquake or

Table 11: Mean computation times for simulation exercise 2

	NxT = **8x512**	**16x512**	**8x1024**	**16x1024**	**8x2048**	**16x2048**
DbC 1	0.021	0.028	0.027	0.038	0.044	0.067
2	0.036	0.049	0.043	0.060	0.062	0.087
4	0.066	0.092	0.067	0.094	0.081	0.115
8	0.125	0.180	0.126	0.181	0.129	0.186
DbC-α 1	0.031	0.108	0.044	0.200	0.084	0.463
2	0.046	0.137	0.064	0.237	0.103	0.496
4	0.086	0.280	0.087	0.276	0.123	0.505
8	0.170	0.585	0.171	0.595	0.173	0.602
SLEXbC	0.355	0.517	0.736	1.095	1.681	2.506

Table 12: Mean computation times for simulation exercise 3

	τ = **0.4**	τ = **0.3**	τ = **0.2**
DbC 1	0.031	0.030	0.030
2	0.047	0.047	0.048
4	0.074	0.074	0.074
8	0.140	0.140	0.140
DbC-α 1	0.066	0.062	0.063
2	0.083	0.093	0.094
4	0.120	0.121	0.120
8	0.235	0.234	0.235
SLEXbC	0.733	0.685	0.675

Figure 5: Real data examples and its curves

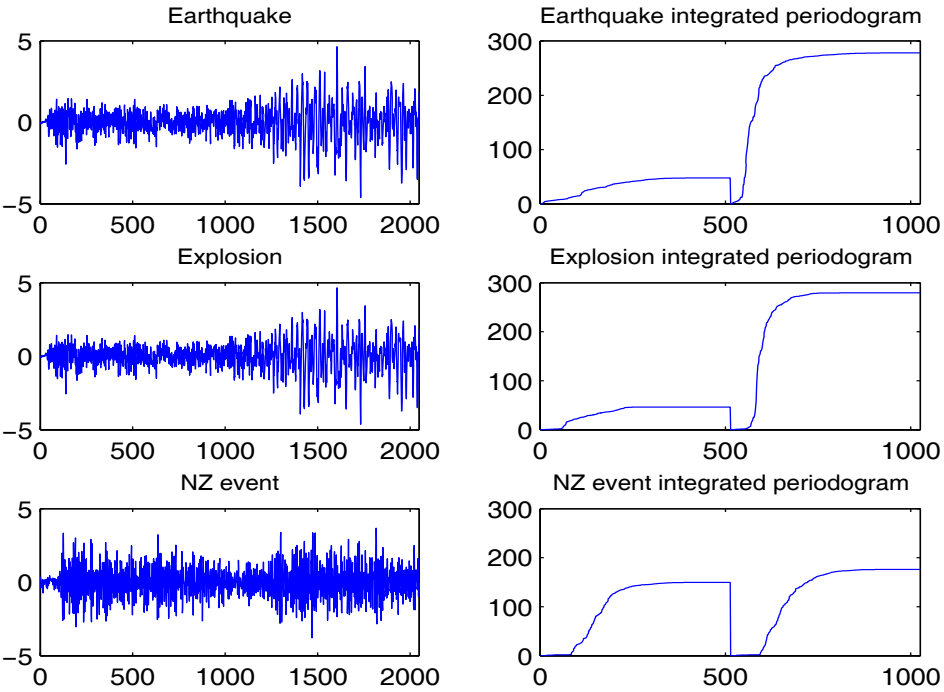

an explosion). This data set was constructed by Blandford (1993). Each series contents 2048 points, and its plot clearly shows two different parts — the first half is the part P and the second half is S. This division is an assumption considered by most authors, and it is based on geological reasons. It is also frequent to consider that both parts are stationary. Kakizawa et al. (1998) give a list of these measurements. Shumway and Stoffer (2000) included a detailed study of this data set, and provide access to the data set in the web site of their book: `http://www.stat.pitt.edu/stoffer/tsa.html`. Figure 5 presents examples of earthquake and explosion, plus the NZ event.

Following the simple criterion given in section 2 to choose between normalized and nonnormalized versions of the cumulative periodogram, and after visual observation of these curves, for each series we have considered the curve formed by merging the nonnormalized integrated periodograms of parts P and S independently computed. That is, we take $k = 2$ as it is suggested by data (and used by most authors). Let us consider the 8 earthquakes as group 1 and the eight explosions as group 2. We have used leave-one-out cross validation to classify the elements of these two groups: that is, removing a series at a time, using the rest of the data set to train the method and finally classifying the removed series. By doing this, both of our algorithms misclassify the first series of the group 2 (explosions). Respecting the NZ event, if we use the previous groups as training sets, both algorithms agree on assigning it to the explosions group, as other authors do, for example, Kakizawa et al. (1998) and Huang et al. (2004).

Now we perform an additional exercise. We consider an artificial data set constructed by the eight earthquakes plus the NZ event as group 1, and the eight explosions as group 2. Note that

our method and most of the published papers classify NZ as an explosion. Then we could consider this artificial suite as a case where some atypical observation is presented in group 1. In this situation, the results using our algorithm 1 are that it misclassifies the first and the third elements of group 2 (explosions), not only the first. But again algorithm 2 misclassifies only the first series of group 2. This seems to show the robustness of our second algorithm. Obviously, as we are using leave-one-out cross validation, both algorithms classifies the NZ event in the explosions group, as we mentioned in the previous paragraph.

6 Conclusions

We define a new time series classification method based on the integrated periodograms of the series (so it is a frequency domain approach). When series are nonstationary, they are split into blocks and the integrated periodograms of the blocks are merged to construct a curve; this idea relays on the assumption of local stationarity of the series. Since the integrated periodogram is a function, the statistical concepts of this type of data can be applied. New series are assigned to the class minimizing the distance between its group mean of curves and the curve of the new data. Since the group mean can be affected by the presence of atypical observations, to add robustness to the classification we proposed substituting the mean curve by the α-trimmed mean, where for each group only the deepest elements are averaged. We evaluate our proposal in different scenarios. We run three simulations exercises containing several models and parameters values, one with stationary series and the other with two types of nonstationarity. After running the exercises without contamination, we repeat all comparisons three more times using exactly the same series but one (the contamination series). We consider one kind of weak contamination and two strong contaminations. We also illustrate the performance of our procedure in a benchmark real data set. Our proposal provides small error rates, robustness and a good computational behavior, what makes the method suitable to classify long time series. Finally, this paper suggests the integrated periodogram contents information useful to classify time series.

Acknowledgements

This research has been supported by CICYT (Spain) grants SEJ2005-06454 and SEJ2007-64500. The first author also acknowledges the support of "Comunidad de Madrid" grant CCG07-UC3M/ HUM-3260.

References

[1] Abraham, C., P.A. Cornillon, E. Matzner-Løber and N. Molinari (2003). Unsupervised Curve Clustering using B-Splines. *Scandinavian Journal of Statistics*. 30 (3), 581–595.

[2] Blandford, R.R. (1993). Discrimination of Earthquakes and Explosions at Regional Distances Using Complexity. *Report AFTAC-TR-93-044 HQ*, Air Force Technical Applications Center, Patrick Air Force Base, FL.

[3] Chandler, G., and W. Polonik (2006). Discrimination of Locally Stationary Time Series Based on the Excess Mass Functional. *Journal of the American Statistical Association*. 101 (473), 240–253.

[4] Ferraty, F., and P. Vieu (2003). Curves Discrimination: A Nonparametric Functional Approach. *Computational Statistics and Data Analysis*. 44, 161-173.

[5] Hall, P., D.S. Poskitt and B. Presnell (2001). A Functional Data-Analytic Approach to Signal Discrimination. *Technometrics*. 43 (1), 1-9.

[6] Hastie, T., A. Buja and R.J. Tibshirani (1995). Penalized Discriminant Analysis. *The Annals of Statistics*. 23 (1), 73-102.

[7] Hirukawa, J. (2004). Discriminant Analysis for Multivariate Non-Gaussian Locally Stationary Processes. *Scientiae Mathematicae Japonicae*. 60 (2), 357–380.

[8] Huang, H., H. Ombao and D.S. Stoffer (2004). Discrimination and Classification of Nonstationary Time Series Using the SLEX Model. *Journal of the American Statistical Association*. 99 (467), 763–774.

[9] James, G.M., and T. Hastie (2001). Functional Linear Discriminant Analysis for Irregularly Sampled Curves. *Journal of the Royal Statistical Society*. Series B, 63, 533-550.

[10] James, G.M., and C. A. Sugar (2003). Clustering for Sparsely Sampled Functional Data. *Journal of the American Statistical Association*. 98 (462), 397-408.

[11] Kakizawa, Y., R.H. Shumway and M. Taniguchi (1998). Discrimination and Clustering for Multivariate Time Series. *Journal of the American Statistical Association*. 93 (441), 328-340.

[12] López-Pintado, S., and J. Romo. (2006). Depth-Based Classification for Functional Data. *DIMACS Series in Discrete Mathematics and Theoretical Computer Science*, American Mathematical Society. Vol. 72.

[13] López-Pintado, S., and J. Romo (2008). On the Concept of Depth for Functional Data. *Journal of the American Statistical Association*, In press.

[14] Maharaj, E.A., and A.M. Alonso (2007). Discrimination of Locally Stationary Time Series Using Wavelets. *Computational Statistics and Data Analysis*. 52, 879–895.

[15] Ombao, H.C., J.A. Raz, R. von Sachs and B.A. Malow (2001). Automatic Statistical Analysis of Bivariate Nonstationary Time Series. *Journal of the American Statistical Association*. 96 (454), 543-560.

[16] Priestley, M. (1965). Evolutionary Spectra and Nonstationary Processes. *Journal of the Royal Statistical Society*. Series B, 27 (2), 204-237.

[17] Sakiyama, K., and M. Taniguchi (2004). Discriminant Analysis for Locally Stationary Processes. *Journal of Multivariate Analysis*. 90, 282–300.

[18] Shumway, R.S. (2003). Time-Frequency Clustering and Discriminant Analysis. *Statistics & Probability Letters*. 63, 307–314.

[19] Shumway, R.H., and D.S. Stoffer (2000). *Time Series Analysis and Its Applications*. New York: Springer.

[20] Taniguchi, M., and Y. Kakizawa (2000). *Asymptotic Theory of Statistical Inference for Time Series*. New York: Springer.